

Electronic Supplementary Information

A Donor-Acceptor Conjugated Polymer-Based nanoparticle for Highly Effective Photoacoustic Imaging and Photothermal Therapy in NIR-II Window

Zuwu Wei^{a,b,c}, Fuli Xin^d, Jian Zhang^e, Ming Wu^{a,b,c}, Ting Qiu^e, Yintao Lan^e,
Shuangying Qiao^f, Xiaolong Liu^{a,b,c*}, and Jingfeng Liu^{a,b,c,d*}

^aThe United Innovation of Mengchao Hepatobiliary Technology Key Laboratory of Fujian Province, Mengchao Hepatobiliary Hospital of Fujian Medical University, Fuzhou 350025, P.R. China

^bMengchao Med-X Center, Fuzhou University, Fuzhou 350116, P. R. China

^cThe Liver Center of Fujian Province, Fujian Medical University, Fuzhou 350025, P.R. China

^dLiver Disease Center, the First Affiliated Hospital of Fujian Medical University, Fuzhou 350005, P.R. China

^eSchool of Basic Medical Science, Affiliated Stomatology Hospital of Guangzhou Medical University, Guangzhou Medical University, Guangzhou 511436, P. R. China

^fSchool of Life Sciences, Fujian Agriculture and Forestry University, Fuzhou 350002, P.R. China

Experiments

Materials

DSPE-PEG2000-N₃ was obtained from Xi'an ruixi Biological Technology Co.,Ltd. 4,7-dibromobenzo[1,2-c:4,5-c']bis([1,2,5]thiadiazole) was purchased from Wuxi Senior Material Co. Ltd. 3-(2-octyl-dodecyl)-thiophene was obtained from Derthon OPV Co Ltd. Pd₂(DBA)₃ and P(tolyl)₃ were bought from Sigma Aldrich Co., Ltd. Aptamer sequences listed in Table 1 were purchased from Sangon Biotech (Shanghai) Co., Ltd. DAPI and CCK-8 were provided by Dojindo Molecular Technologies. LIVE/DEAD[®] Viability/Cytotoxicity Kit and Annexin V-Fluoroisothiocyanate (FITC)/propidium iodide (PI) apoptosis detection kit were purchased from Invitrogen. All the reactions were carried out under argon atmosphere.

Table 1. Sequences of the TLS11a and control aptamer.

Aptamer	Target	Length	Sequence
TLS11a	Hepatocellular carcinoma	63 n.t.	ACAGCATCCCCATGTGAACAATCGCATT GTGATTGTTACGGTTTCCGCCTCATGGAC GTGCTG-(C3)-DBCO
TD4R	Negative	63 n.t.	ATCCGTCACACCTGCTCTTGACACGCGT ACGGGTCCGGACATGTCATAACGGACTG GTGTTGG-(C3)-DBCO
TLS11a-Cy3	Hepatocellular carcinoma	63 n.t.	Cy3- ACAGCATCCCCATGTGAACAATCGCATT GTGATTGTTACGGTTTCCGCCTCATGGAC GTGCTG-(C3)-DBCO
TD4R-Cy3	Negative	63 n.t.	Cy3- ATCCGTCACACCTGCTCTTGACACGCGT ACGGGTCCGGACATGTCATAACGGACTG GTGTTGG-(C3)-DBCO

Synthesis of conjugated polymer PBBTDTS

3-(2-octyl-dodecyl)-thiophene (3.48 g, 9.54 mmol) was dissolved in anhydrous THF (75 mL). After the reaction system cooling down to -78 °C, LDA (2.0 M in THF/heptane/ethylbenzene, 5.3 mL, 10.59 mmol) was dropwise injected to the mixture and kept the solution temperature at -78 °C for 1 h. Trimethyltinchloride solution (1.0 M in hexane, 10.95 mL, 10.95 mmol) was then rapidly added to the mixture. Then the system was stirred 12 h at room temperature (R.T). Afterwards, the reaction was quenched by D.I. water and extracted with diethyl ether. The organic layer was dried over anhydrous MgSO₄, filtered and concentrated under reduced pressure to obtain yellow oil compound (4.53 g, 89.9%).¹ The compound trimethyl-[4-(2-octyl-dodecyl)-thiophen-2-yl]-stannane was applied to the next reaction without further purification.

4,7-dibromobenzo[1,2-c:4,5-c']bis([1,2,5]thiadiazole) (0.55 g, 1.56 mmol),

trimethyl-[4-(2-octyl-dodecyl)-thiophen-2-yl]-stannane (1.5 g, 2.82 mmol) and Pd(PPh₃)₄ (120 mg, 0.1 mmol) were dissolved in 100 mL of toluene. After the mixture was refluxed for 1 day, Pd(PPh₃)₄ (120 mg, 0.1 mmol) and trimethyl-[4-(2-octyl-dodecyl)-thiophen-2-yl]-stannane (1.5 g, 2.82 mmol) were then added into the solution again. Afterwards, the solution was allowed to react for 1 more day. Then, the reaction system was cooled down to R.T and the solvent was eliminated through rotary evaporation. The crude product was purified by column chromatography (SiO₂, hexane:DCM, 1:1) to obtain the product (0.71 g). ¹H NMR (CDCl₃, 600 MHz): δ (ppm) 8.72 (s, 2H), 7.23 (s, 2H), 2.708 (d, 4H), 1.77 (m, 2H), 1.29 (m, 64H), 0.869 (m, 12H) (Fig. S2). ¹³C NMR (CDCl₃): δ (ppm) 14.128, 22.703, 26.703, 29.386, 29.765, 30.139, 31.936, 33.397, 34.936, 38.995, 113.132, 127.121, 134.593, 136.996, 142.778, 150.903 (Fig. S3). **ESI MS**: 919.58 ([M + H]⁺) (Fig. S4).

4,7-bis-[4-(2-octyl-dodecyl)-thiophen-2-yl]-benzobisthiadiazole (0.6 g, 0.65 mmol) and NBS (300 mg, 16.86 mmol) were dissolved in THF (35 mL). Then, the reaction system was stirred 12 h at R.T. After eliminate of solvent, the solid was dissolved into small amount of DCM. Afterwards, the solution was dropwise added into huge amount of methanol.² The precipitate 4,7-bis-[5-bromo-4-(2-octyl-dodecyl)-thiophen-2-yl]-benzobisthiadiazole was collected and dried under vacuum (0.63 g). ¹H NMR (CDCl₃, 600 MHz): δ (ppm) 8.265 (s, 2H), 2.537 (d, 4H), 1.776 (m, 2H), 1.301 (m, 64H), 0.869 (m, 12H) (Fig. S5). ¹³C NMR (CDCl₃): δ (ppm) 14.135, 22.730, 26.621, 29.416, 29.480, 29.7785, 29.819, 31.959, 33.415, 38.597, 111.560, 118.018, 133.8, 136.894, 141.996, 149.986 (Fig. S6). **ESI MS**: 1075.71 ([M + H]⁺) (Fig. S7).

4,7-bis-[5-bromo-4-(2-octyl-dodecyl)-thiophen-2-yl]-benzobisthiadiazole (150 mg, 0.16 mmol), 4,4'-Bis(octyl)-5,5'-bis(trimethyltin)-dithieno[3,2-b:2',3'-d]silole (119 mg, 0.16 mmol), Pd₂(DBA)₃ (10 mg), and P(tolyl)₃ (40 mg) were dissolved in 10 mL toluene and then refluxed for 48 h. After cooling down to R.T, 100 mL of CH₃OH was injected, and the precipitate was collected by filtration, then purified with Soxhlet extraction using CH₃OH, CH₂Cl₂, sequentially.² The CH₂Cl₂ fraction was concentrated and reprecipitated with CH₃OH. The kermesinu solid was gathered and dried under vacuum.

Preparation of polymer nanoparticles (BD NPs)

The BD nanoparticles were prepared by nanoprecipitation method. 1 mg of conjugated polymer PBBTDTS and 20 mg of DSPE-PEG₂₀₀₀-N₃ were completely dissolved in 2 mL THF and sonicated for 5 min at R.T. Subsequently, the solution was rapidly injected into 10 mL Deionised (DI) water under vigorous stirring. Then, the system was further stirred under R.T for 12 h to evaporate the THF, and then ultra-filtered again at a speed of 4000 rpm for 0.5 h to remove free DSPE-PEG₂₀₀₀-N₃ to obtain the BD NPs.

Aptamer-Nanoparticle Conjugation.

In order to obtain aptamer-modified polymer nanoparticles, the pre-prepared BD NPs were dispersed in PBS at pH 7.4. Then, an excess amount of DBCO-labeled aptamer was injected to the mixture dispersion and further shake 1 h at R.T. Then the mixture followed by three washings with PBS using ultrafiltration at 4000 rpm to remove any aptamer that did not conjugate to the BP NPs. The obtained BDA NPs were dispersed in PBS and stored at 4 ° C for further usage.

The BDN NPs were prepared by the same method, but with control aptamer to instead of targeting aptamer. To evaluate the cellular uptake ability of BDA and BDN, the aptamer-Cy3 and control-aptamer-Cy3 was doped into nanoparticles to obtain BDA-Cy3 and BDN-Cy3 NPs. The fluorescence spectrum certified the successful modification of aptamer (Fig. S8).

Characterization

¹H NMR spectra were performed by Bruker Ultrashield 500 Plus NMR spectrometer. UV-Vis-NIR spectra was performed on a Cary 5000 UV-Vis-NIR spectrophotometer. Dynamic light scattering (DLS) was carried out by Zetasizer Nano ZS. TEM image was provided by transmission electron microscopy with an accelerating voltage of at 200 kV. Laser-confocal scanning imaging of HepG-2 cells was performed by confocal microscope Zeiss LSM780. The photoacoustic properties of BDA NPs were analyzed by a home-made multi-spectral photoacoustic microscopy system.

Photothermal effect and photostability of BDA NPs under 1064 nm laser irradiation

The aqueous dispersion of BDA NPs (1 mL) with different concentrations (0, 2.5, 5.0, 10, 20, 40 and 80 $\mu\text{g}\cdot\text{mL}^{-1}$) in cuvette was irradiated by a 1064 nm laser (1 W/cm^2) for 10 min. The changes of temperature were recorded by a thermocouple microprobe ($\phi = 0.5$ mm). Then, the photostability of BDA NPs was investigated under the photothermal heating and nature cooling cycles by the 1064 nm laser irradiation at the power density of 1.0 $\text{W}\cdot\text{cm}^{-2}$. To study the photothermal conversion efficiency, 1 mL BDA nanoparticles (40 $\mu\text{g}/\text{mL}$) in a plastic vial was irradiated for 15 min with a 1064 nm laser (1 $\text{W}\cdot\text{cm}^{-2}$). The temperature was monitored during 15 min irradiation when the temperature achieved a steady-state, followed by the subsequent naturally cooling to R.T. The photothermal conversion efficiency (η) was calculated using the reported method.

Photoacoustic properties of BDA NPs under 1064 nm laser irradiation

The photoacoustic properties of BDA NPs were evaluated by a home-made multi-spectral photoacoustic microscopy system. Firstly, to investigate the photoacoustic imaging ability, the aqueous solution of BDA NPs with different concentrations (0, 2.5, 5.0, 10, 20, 40 and 80 $\mu\text{g}\cdot\text{mL}^{-1}$) were injected into an optical and acoustically transparent silicon tube with a diameter of 1 mm. These tubes were placed parallel to each other in concentration order and fixed in agar. Then, the photoacoustic imaging was monitored at 1064 nm.³

Cell Culture

HepG-2 cells were provided by the American Type Culture Collection (ATCC). HepG-2 cells were cultured in DMEM with 10% FBS and 1% antibiotics (penicillin–streptomycin) (Corning) in a humidified environment which contains 5% CO_2 and 95% air at 37 $^\circ\text{C}$.⁴

Cellular internalization analysis

To evaluate the intracellular uptake ability of BDA nanoparticles, the HepG-2 cells were cultured in the CLSM dishes and adhered for 24 h. Then, the experiments were randomly divided into following three groups: (1) Control, (2) BDA-Cy3, (3) BDN-

Cy3. After different time point (2 or 4 h), the cells were washed with fresh PBS for 3 times, and then fixed by 4% formaldehyde for 10 min. Afterwards, the cell nuclei were stained by DAPI (5 μ M) for 10 min. Finally, the cells were imaged by Confocal laser scanning microscopy.⁵

***In Vitro* PTT Therapy**

BDA NPs in PBS were diluted to various concentrations using DMEM. Then, the HepG-2 cells were inoculated in 96-well plates and divided into four groups: (1) BDA, (2) BDA+1064 nm, (3) BDN+1064 nm and (4) BDA+HepG-2 pre-treated by aptamer+1064 nm. After 4 hours, the cell culture medium was replaced by 50 μ L fresh medium. Then, the group (1) was maintained in darkness, while other groups were irradiated for 5 min using 1064 nm laser with 0.8 W \cdot cm⁻² power. Afterwards, the cells were further cultured at 37 $^{\circ}$ C with 5% CO₂ and 95% air for 24 h. Finally, the cell culture medium was substituted by 100 μ L 10% CCK-8 medium and then further incubated the cells at 37 $^{\circ}$ C for 2 h. After that, the absorbance (450 nm) was detected using Molecular Devices. The cell viability was obtained using the reported method.⁵

Live/Dead Cell Staining Assay

HepG-2 cells were inoculated in 96-well plates (5×10^4 cells per well) and divided into six groups: (1) Control, (2) BDA NPs, (3) Laser only, (4) BDN+1064 nm; (5) BDA+HepG-2 pre-treated by free aptamer+1064 nm and (6) BDA+1064 nm. After 1064 nm irradiation, the cells were cultured at 37 $^{\circ}$ C with 5% CO₂ and 95% air for 24 hours. Finally, the fresh DMEM medium containing LIVE/DEAD[®] Viability/Cytotoxicity Kit was added in all cells and further cultured for 15 min. Eventually, the cells were observed and record through fluorescence microscope.⁵

Apoptosis Evaluation by Flow Cytometry

HepG-2 cells were cultured in 6-well plates (3×10^5 cells per well). After 24 h culture, the cells were divided into six groups: (1) Control, (2) BDA, (3) 1064 nm, (4) BDN+1064 nm; (5) BDA +HepG-2 pre-treated by aptamer+1064 nm and (6) BDA+1064 nm. After 1064 nm irradiation, the cells were further incubated for 24 hours in cell incubator. Afterwards, all the cells were washed by fresh PBS (3 times), digested and then collected by centrifugation. After being further washed with PBS (3 times),

the cells were dispersed in 500 μ L of annexin binding buffer. After that, all cells were dyed by PI or Annexin-V-FITC about 15 min and finally recorded by flow cytometry.⁵

Live Subject Statement

All animal experiments were performed strictly under the guidelines of the National animal management regulations of China and the animal study guidelines of Fujian Medical University, as well as approved by the Animal Ethics Committee of Mengchao Hepatobiliary Hospital of Fujian Medical University.

In Vivo Photoacoustic imaging

To evaluate the *in vivo* photoacoustic performance of BDA or BDN NPs for HepG-2 subcutaneous tumor imaging, mice bearing subcutaneous tumor were anesthetized with sodium pentobarbital (1 %), and restrained in a holder designed specifically for photoacoustic imaging. Before BDA or BDN NPs injection, the photoacoustic images of the tumor site were captured first as control by the home-made multi-spectral photoacoustic microscopy system.⁵ The photoacoustic images of the tumor site were imaged before and 4, 8, 12 and 24 h after intravenous injection of BDA or BDN NPs.

In Vivo PTT Therapy

The balb/c nude mice bearing HepG-2 tumors were randomly divided into 5 groups with five mice per group as follows: (1) Control (mice were only intratumorally injected with PBS), (2) BDA NPs, (3) 1064 nm laser, (4) BDN + 1064 nm laser and (5) BDA + 1064 nm laser. Mice bearing HepG-2 tumors were intravenously injected with 100 μ L (4.0 mg/mL) of nanoparticles, and mice treated with the same volume of saline were used as the control. After 12 h of NPs injection, the mice were irradiated 10 min by 1064 nm laser with 1 W cm^{-2} power. Meanwhile, the temperature changes at the tumor sites in group 3-5 were performed using a thermal camera during the irradiation. The body weight and the tumor volume of the mice were detected every 3 days. In addition, the hematoxylin and eosin (H&E), the immunofluorescence staining as well as TUNEL were performed to investigate the tissue destruction and cell apoptosis after therapy.⁶

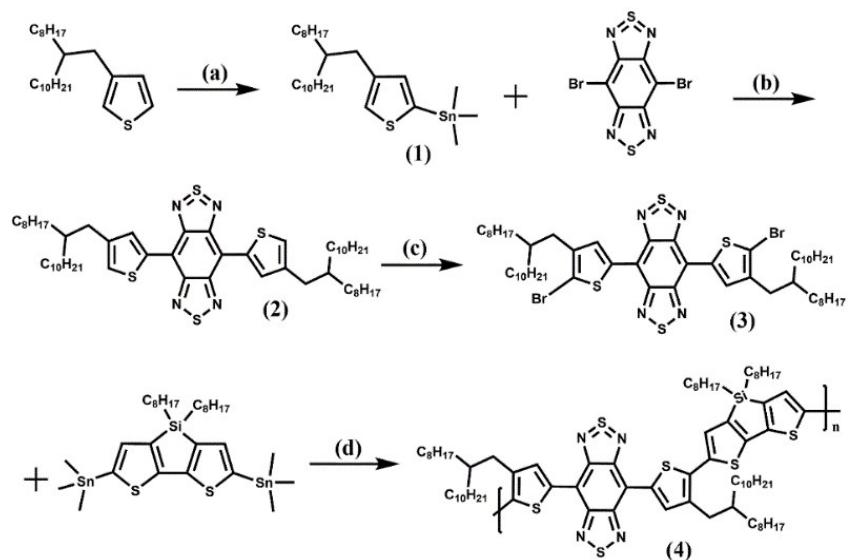


Fig. S1 Synthetic routes of PBBTDS. Reagents and conditions: (a) LDA, THF, $-78\text{ }^\circ\text{C}$; (b) $\text{Pd}(\text{PPh}_3)_4$, Toluene, $110\text{ }^\circ\text{C}$; (c) NBS, THF, $0\text{ }^\circ\text{C}$; (d) $\text{Pd}_2(\text{DBA})_3$, $\text{P}(\text{o-tolyl})_3$, Toluene, $110\text{ }^\circ\text{C}$.

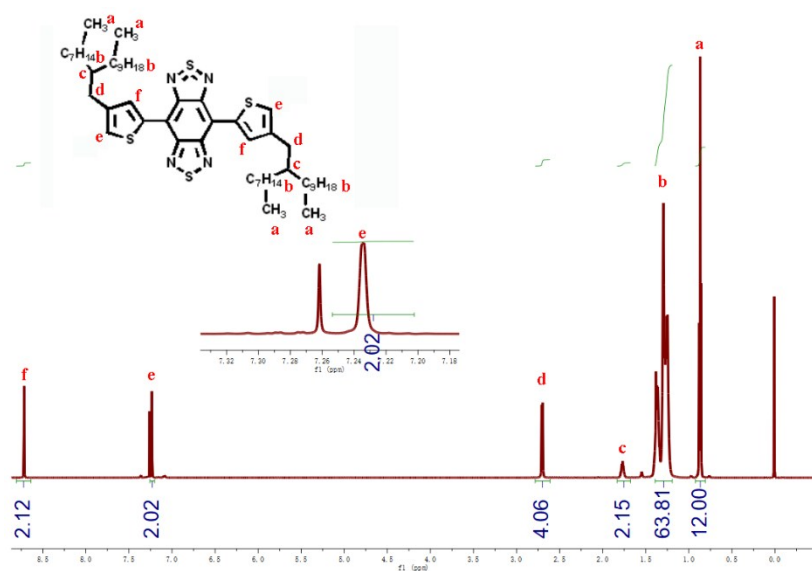


Fig. S2 ^1H NMR spectrum of compound (2).

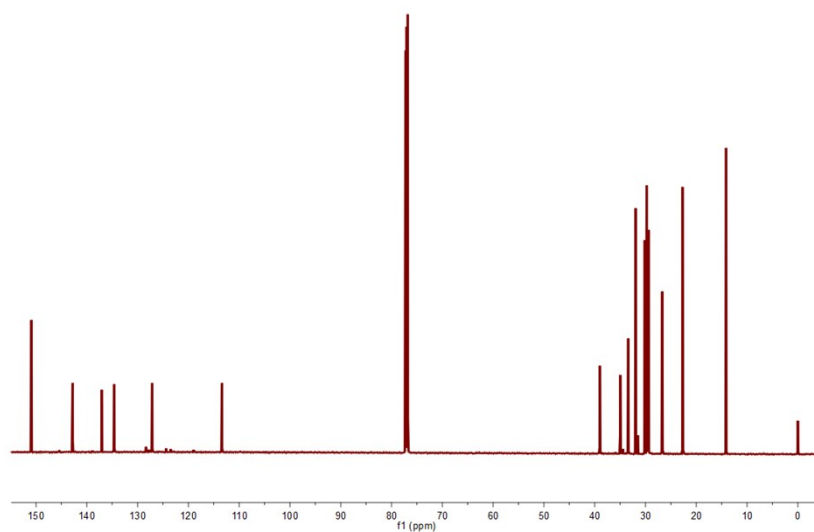


Fig. S3 ^{13}C NMR spectrum of compound (2).

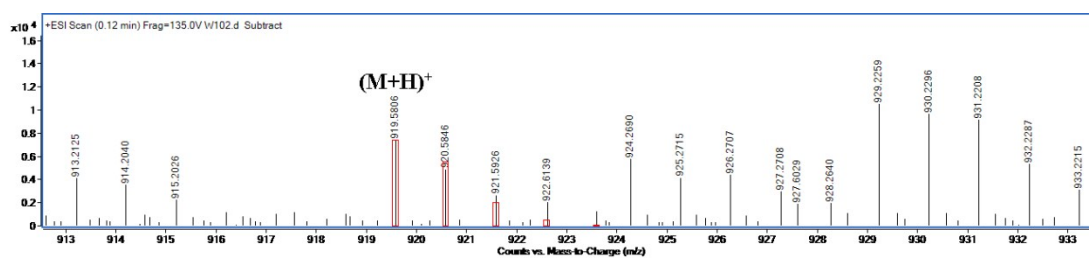


Fig. S4 ESI spectrum of compound (2).

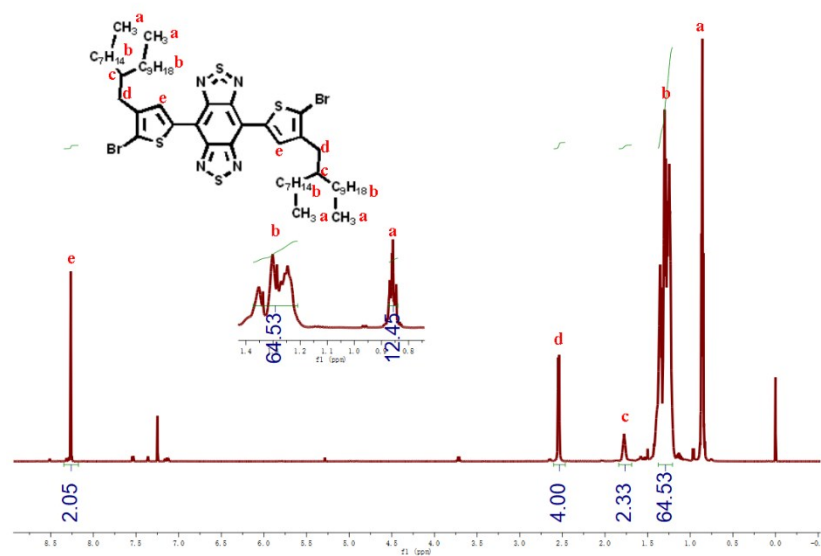


Fig. S5 ^1H NMR spectrum of compound (3).

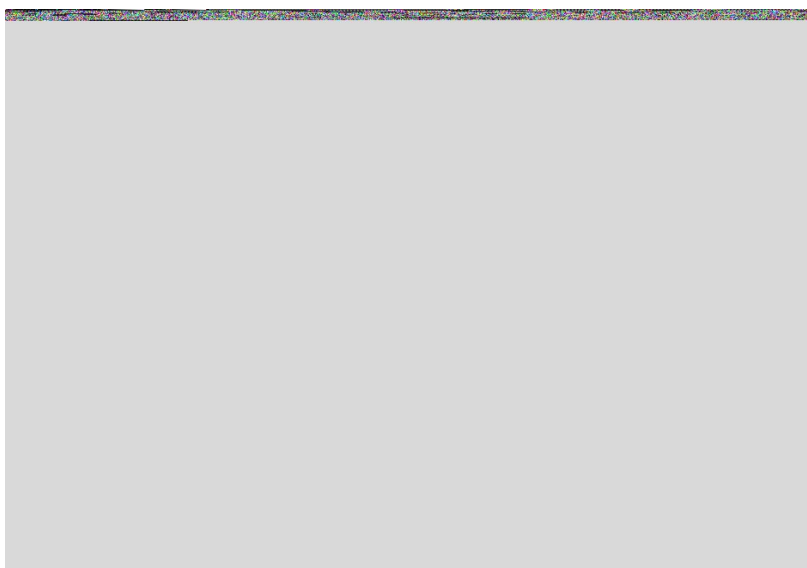


Fig. S6 ^{13}C NMR spectrum of compound (3).

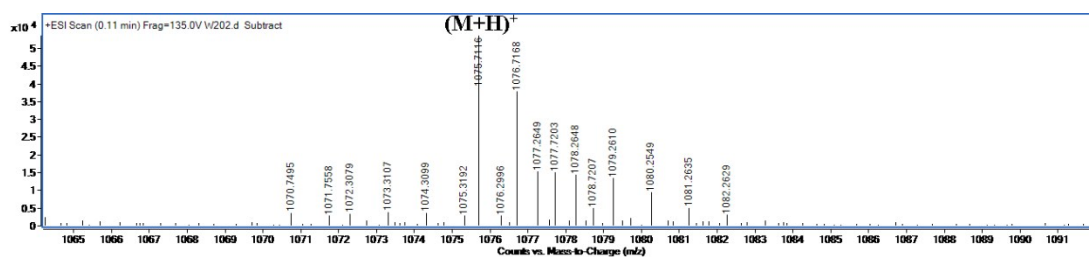


Fig. S7 ESI spectrum of of compound (3).

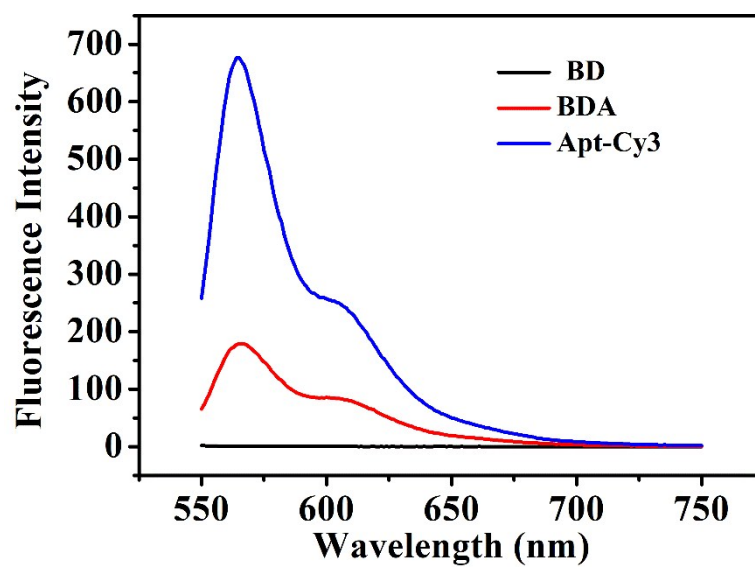


Fig. S8 The fluorescence spectra of BD, BDA and Apt-Cy3.

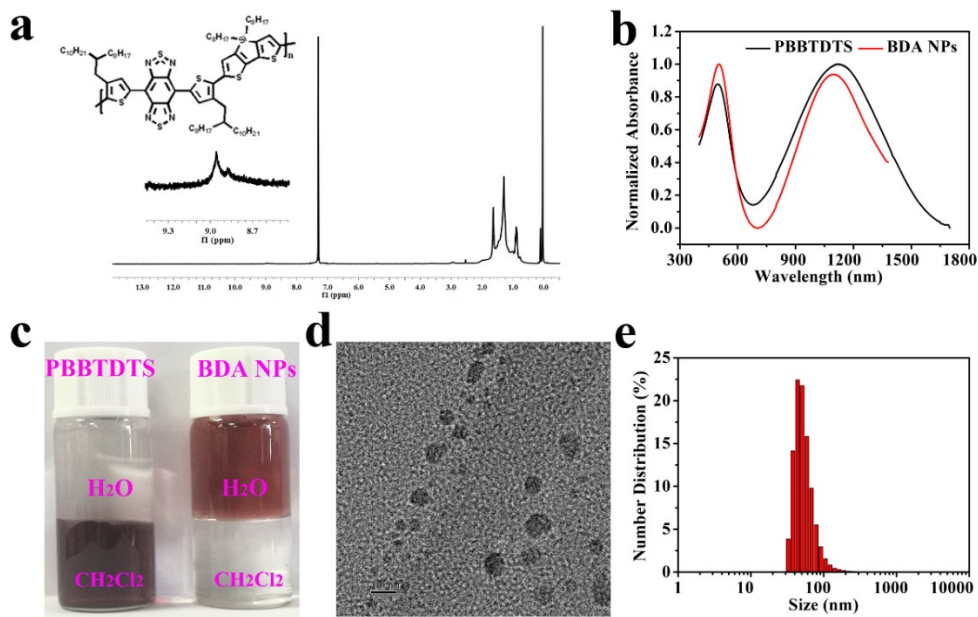


Fig. S9 a) The ^1H NMR spectrum of PBBDTDS. b) UV-Vis-NIR absorption spectra of PBBDTDS in CH_2Cl_2 and BDA NPs in H_2O . c) the picture of PBBDTDS or BDA NPs in $\text{H}_2\text{O}/\text{CH}_2\text{Cl}_2$. d) Transmission electron microscope image of BDA NPs. Scale bar is 10 nm e) Dynamic light scattering size distribution of BDA NPs.

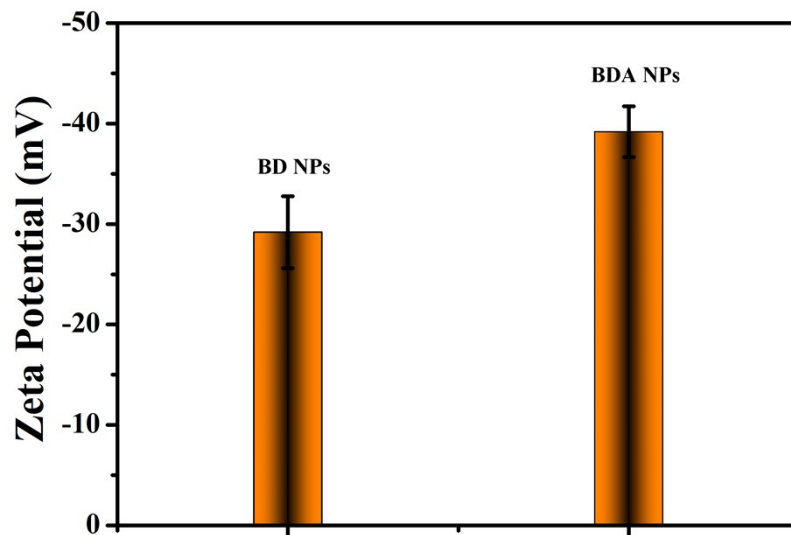


Fig. S10 The Zeta potential of BD and BDA NP dispersion in water.

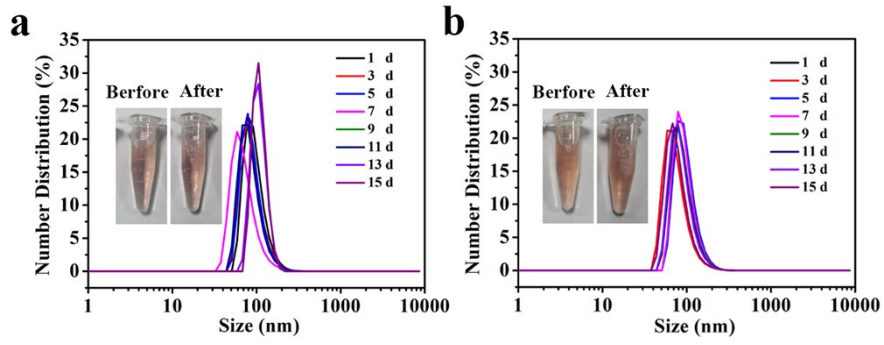


Fig. S11 Size distributions of BDA nanoparticles in (a) PBS, (b) PBS with 10% FBS measured by DLS.

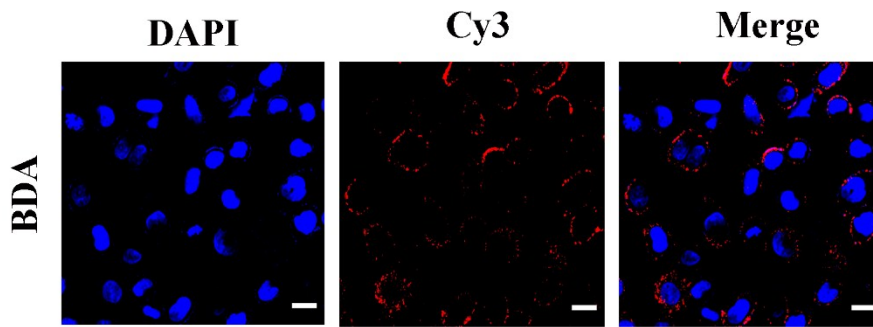


Fig. S12 Confocal laser scanning microscopy of HeLa cells incubated with BDA NPs for 4 h.

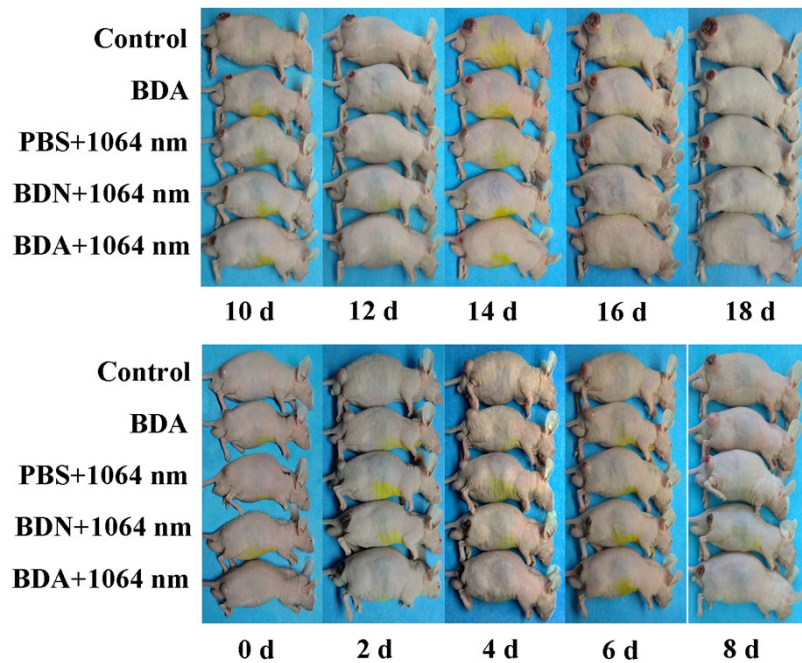


Fig. S13 Representative pictures of mice with different treatment.

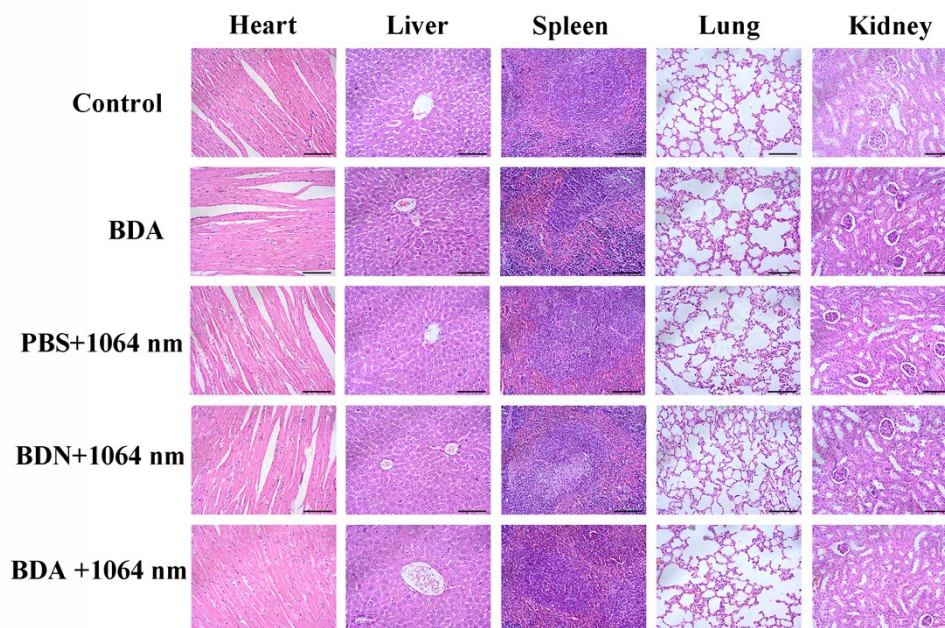


Fig. S14 H&E staining of heart, live, spleen, lung, and kidney of mice after indicated treatments for 18 days.

References

1. J. H. Yun, H. Ahn, P. Lee, M. J. Ko and H. J. Son, *Macromolecules*, 2017, **50**, 7567-7576.
2. J. Fan, J. D. Yuen, M. Wang, J. Seifert, J. H. Seo, A. R. Mohebbi, D. Zakhidov, A. Heeger and F. Wudl, *Adv. Mater.*, 2012, **24**, 2186-2190.
3. J. Zhang, H. Chen, T. Zhou, L. Wang, D. Gao, X. Zhang, Y. Liu, C. Wu and Z. Yuan, *Nano Res.*, 2017, **10**, 64-76.
4. J. Zeng, M. Wu, S. Lan, J. Li, X. Zhang, J. Liu, X. Liu, Z. Wei and Y. Zeng, *J. Mater. Chem. B*, 2018, **6**, 7889-7897.
5. Z. Wei, M. Wu, S. Lan, J. Li, X. Zhang, D. Zhang, X. Liu and J. Liu, *Chem. Commun.*, 2018, **54**, 13599-13602.
6. M. Wu, X. Y. Lin, X. H. Tan, J. Li, Z. W. Wei, D. Zhang, Y. S. Zheng, A. X. Zheng, B. X. Zhao, Y. Y. Zeng, X. L. Liu and J. F. Liu, *ACS Appl. Mater. Interfaces*, 2018, **10**, 19416-19427.